# Computational Physics Term Project, Task 1: Proposal
A Multi-Dimensional, Distributed, Non-Oscillatory Ideal Magnetohydrodynamics Framework

Neil Baker[1], C. Michael Haynes[2], Corinne Hill[3], Eden Schapera[1], Kenneth Thompson[3]

[1]School of Physics, Georgia Institute of Technology, Atlanta, GA, USA
[2]School of Earth and Atmospheric Sciences, Georgia Institute of Technology, Atlanta, GA, USA
[3]George W. Woodruff School of Mechanical Engineering: Nuclear and Radiological Engineering, Georgia Institute of Technology, Atlanta, GA, USA

SDO/AIA 171 2013-04-09 14:15:12 UT
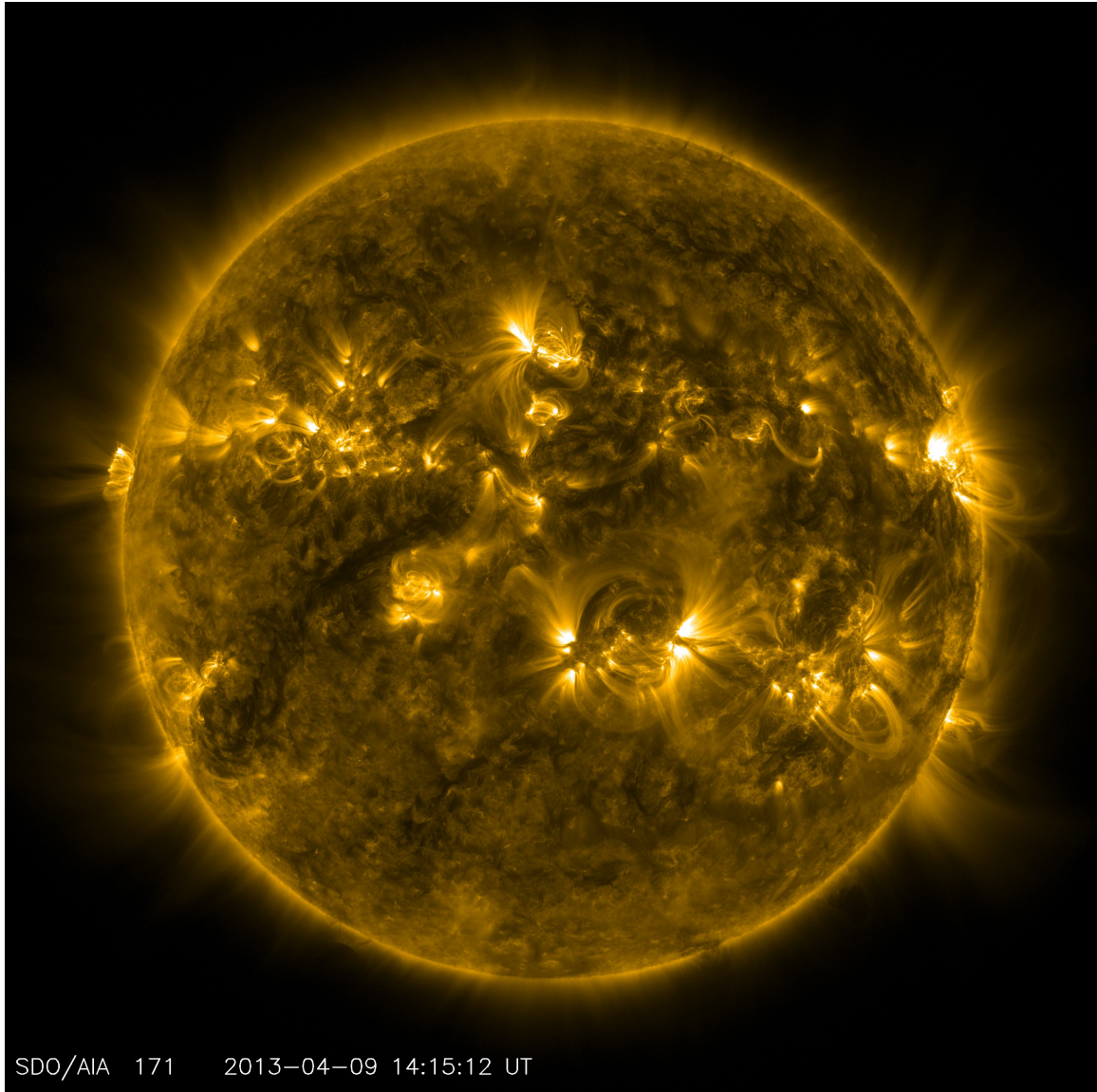
1 Background and Motivation

1.1 Magnetohydrodynamics Framework

We will work to derive the Magnetohydrodynamics (MHD) equations formally prior to discussing some wave structure of the MHD equations that will be important considerations for our Courant-Friedrichs-Lewy (CFL) criteria. For details about the formulation of ideal MHD, see (Baumjohann & Treumann, 1999). We first start from the general case for a many body system with distribution function f_α in 6-dimensional phase space (3 momentum and 3 position). We then utilize a mean theory by assuming that the fields and forces are averaged over many particles and hence are macroscopic. The exact particle locations can be expressed through a generic collision term that changes the particle trajectories. This is given as

$$\partial_t f + \mathbf{u} \cdot \nabla_r f + \frac{\mathbf{F}}{m}\nabla_v f = \left(\frac{\delta f}{\delta t}\right)_{\text{coll}} \tag{1}$$

We define the normalized moment

$$\langle g(\mathbf{r}, t)\rangle = \frac{\int g(\mathbf{r}, \mathbf{u}, t_x)f(\mathbf{r}, \mathbf{u}, t)\,\mathrm{d}\mathbf{u}}{\int f(\mathbf{r}, \mathbf{u}, t)\,\mathrm{d}\mathbf{u}} \quad .$$

we can take the 0th order moment to obtain the number density

$$n(\mathbf{r}, t) = \int f(\mathbf{r}, \mathbf{u}, t)\,\mathrm{d}\mathbf{u} \tag{2}$$

The Lorentz Force acts on charged particles (charge q) in magnetic ($\mathbf{B}$) and electric ($\mathbf{E}$) fields: $\mathbf{F} = q(\mathbf{E} + \mathbf{u} \times \mathbf{B})$. Since $\partial_{\mathbf{u}_i}F_i = 0$, we can write

$$\partial_t(n\langle g\rangle) - n\langle\partial_t g\rangle + \nabla_r n\langle\mathbf{u}g\rangle - \frac{n}{m}\langle\mathbf{F}\nabla_{\mathbf{u}}g\rangle = \int g\left(\frac{\delta f}{\delta t}\right)_{\text{coll}}\mathrm{d}\mathbf{u}$$

(margin, handwritten:) I take your word here. I see how it comes from Eq.1, but can't do the math in my head

letting $g = 1$ we get the equation of continuity

$$\partial_t n(\mathbf{r}, t) + \nabla_r(n(\mathbf{r}, t)\langle\mathbf{u}(\mathbf{r}, t)\rangle) = \int\left(\frac{\delta f}{\delta t}\right)_{\text{coll}}\mathrm{d}\mathbf{u}$$

(margin, handwritten:) ✓

The proposed work considers a regime where the collisional term from equation (1) is 0. For the first moment, $g = m\mathbf{u}$, we have the equation of motion

$$\partial_t(mn(\mathbf{r}, t)\langle\mathbf{u}\rangle) + \sum_j \partial_{x_j}n(\mathbf{r}, t)m\langle u_j\mathbf{u}\rangle - n(\mathbf{r}, t)\langle\mathbf{F}(\mathbf{r}, t)\rangle = \int m\mathbf{u}\left(\frac{\delta f}{\delta t}\right)_{\text{coll}}\mathrm{d}\mathbf{u} \tag{3}$$

we turn our attention towards treatment of the pressure (tensor) for the isotropic case, hidden in the above expression. We write the pressure as $p = nk_BT$, assumed for ideal MHD. Now we turn out attention toward the energy. We take $g = \frac{1}{2}m\mathbf{u}^2$, and using $\frac{1}{2}nm\langle u_i^2\rangle = \frac{1}{2}nm\langle\mathbf{u}\rangle^2 + \frac{3}{2}p$, this yields

(margin, handwritten:) ?

$$\partial_t\left(\frac{nm}{2}\langle\mathbf{u}\rangle^2 + \frac{3}{2}p\right) + \nabla\cdot\left(\left(\frac{nm}{2}\langle\mathbf{u}\rangle^2 + \frac{5}{2}p\right)\langle\mathbf{u}\rangle + \sum_i \Pi_{ij}\langle u_i\rangle + \mathbf{q}\right) = qn\mathbf{E}\cdot\langle\mathbf{u}\rangle + \textcircled{R}\langle\mathbf{u}\rangle + \textcircled{Q} \tag{4}$$

(margin, handwritten:) Undefined — mathbf — resistance?

where $\mathbf{q}$ is the energy-flux density due to random motion and $\mathbf{Q}$ represents the heat generated by collisions. From the above we can note that the left hand side is the total derivative of kinetic energy and internal energy, total pressure and $\mathbf{q}$ term. This along with our previous derivations allows us to write the following energy equation

$$\frac{3}{2}\partial_t p + \nabla\left(\frac{3}{2}p\langle\mathbf{u}\rangle\right) + nT\nabla\langle\mathbf{u}\rangle + \sum_{ij}\Pi_{ij}\partial_{x_j}\langle u_i\rangle + \nabla\mathbf{q} = \mathbf{Q} \tag{5}$$

this can be written for temperature as well. Now the above holds for both the electrons and ions in the gas. We seek to combine these into a single expression. We define the average values

$$\rho = n_e m_e + n_i m_i \qquad \mathbf{u} = \frac{1}{\rho}(n_e m_e \mathbf{u}_e + n_i m_i \mathbf{u}_i) \tag{6}$$

$$\rho_c = -en_e + Zn_i e \qquad \mathbf{J} = -en_e\left(\mathbf{u}_e - \frac{Zn_i}{n_e}\mathbf{u}_i\right) \tag{7}$$

(handwritten: Assumes a single ion species → But this is fine)

(note second ρ_c is the charge density)this immediately allows us to write from our continuity equation

$$\partial_t \rho + \nabla \cdot (\rho \mathbf{u}) = 0 \qquad \partial_t \rho_c + \nabla \cdot \mathbf{J} = 0 \tag{8}$$

Plasmas obey quasi-neutrality ($n_e \approx Zn_i$) and due to the large mass ratio between m_e, m_i, we can write equations (6) and (7) less stringently. For resistive plasmas we can write the collision term (with some work) to be $\mathbf{R} = en_e \eta \mathbf{J}$, where $\mathbf{J}$ is the current density. This leads to the following equation of motion:

(handwritten: \mathbf)

$$\rho \frac{d\mathbf{u}}{dt} = -\sum_\beta \partial_{x_\beta} P_{\alpha\beta} + \rho \mathbf{E} + (\mathbf{J} \times \mathbf{B}) - \rho \nabla \phi_g \tag{9}$$

where $\mathbf{P}_{\alpha\beta} = \mathbf{P}^e_{\alpha\beta} + \mathbf{P}^i_{\alpha\beta}$ and the ϕ_g term represents gravitational force. We can also write our new generalized ohm's law as

$$\mathbf{E} + \left(\mathbf{u} - \frac{\mathbf{J}}{en_e}\right) \times \mathbf{B} + \frac{1}{en_e}\sum_\beta \partial_{x_\beta} P^e_{\alpha\beta} - \eta \mathbf{J} = \frac{m_e}{e^2 n_e}\partial_t \mathbf{J} \tag{10}$$

Thus, equations (5, 8, 9, 10) coupled with Maxwell's equations form the set of equations for MHD. For our case, we consider the ideal MHD regime: that is, we do not consider collisional plasmas, viscosity, resistivity, heat flux, and the equation of state for plasmas takes $\gamma = 2$. Within these assumptions (see section 3.1) we arrive at the system of equations (12-16). This is the system the proposed work will apply and solve computationally to investigate the behavior of plasma. ✓

(handwritten: It's been a long time since I've seen the MHD derivation, so this was nice to read, though dense.)

1.1.1 MHD Waves

Here we briefly describe the eigenstructure and fundamental wave modes for the MHD system. In the above calculation, we ignored the displacement current in Ampere's law, removing electromagnetic waves from the solution. However, magnetic pressure and field line tension as restoring forces. This gives rise to Alfvén Waves, obtained via linearization of the force equation. This yields We will consider two cases: purely compressional and incompressible displacement. For the first case we small density fluctuations in the direction perpendicular to the equilibrium magnetic field lines. We then get the compressional Alfvén wave that acts similar to a sound wave that occurs due to the restoring force of kinetic pressure, with phase velocity

(handwritten: have? consider?)

(handwritten: Never defined β ratio.)

$$u_{\text{ph}} = \sqrt{\gamma \frac{p_0}{\rho_0} + \frac{\mathbf{B}_0^2}{\mu_0 \rho_0}} \quad .$$

the wave will propagate at the speed of sound $c_s = \sqrt{\gamma p_0/\rho_0}$ for large β. For small β, it reduces to the Alfvén speed:

$$v_A = \frac{B_0}{\sqrt{\mu_0 \rho_0}} \quad .$$

In the second case, shear Alfvén waves occur. In this the phase velocity is the Alfvén velocity which plays a large role in setting the natural timescale limited by inertia. There also exists fast and slow magnetosonic waves that are associated to nonzero perturbations in the plasma density and pressure in both the parallel and perpendicular directions. The speeds are

$$V_\pm = \sqrt{\frac{1}{2}\left(V_A^2 + V_S^2 \pm \sqrt{(V_A^2 + V_S^2)^2 - 4V_A^2 V_S^2 \cos^2\theta}\right)}$$

from the linearized MHD equations where

$$V_A = \sqrt{\frac{B_0^2}{\mu_0 \rho_0}} \qquad V_S = \sqrt{\frac{\gamma p_0}{\rho_0}}$$

The fast wave can be interpreted as the compressional-Alfvén wave modified by a non-zero plasma pressure. For the slow mode, fluctuations interfere causing its lower propagation speed.

1.2 Existing Models and Technical Considerations

The relevance of magnetohydrodynamics to many areas of research has motivated scientists to develop computational models of systems that obey the MHD equations (e.g., Stone & Norman, 1992; Jia et al., 2009; Duling et al., 2014; Dorelli et al., 2015). These models help us understand how bulk quantities such as density, velocity, or pressure evolve in time, and help contextualize or interpret data collected in situ. Kinetic codes (e.g., Winske & Omidi, 1996; Lipatov et al., 2005; Fatemi et al., 2016) also exist, as well as hybrid codes (e.g., Müller et al., 2011; Fatemi et al., 2012) that combine MHD with kinetic theory, but for the sake of brevity, they will not be discussed here. Since most plasmas consist of multiple species of varying charges, MHD codes often use a multi-fluid approach. Since our science questions can be addressed within the ideal MHD framework (see section 2), the multi-fluid approach is not needed. Key features of MHD solvers include:

1. **The solver method (finite-differencing, finite-volume, etc.).** In a finite difference scheme, the MHD equations are written out explicitly as a collection of discrete derivative approximations. In a finite-volume scheme, the entire set of MHD equations (see Section 3.3) is effectively reduced to a single conservation equation, which is then integrated over each cell in the grid. In this project, we will employ a finite-volume method. *Nice*

2. **The differentiation scheme (central, upwind, downwind).** In a central differencing scheme, a derivative of some quantity at position i is calculated using the value of that quantity at position $i-1$ and $i+1$ from the previous time step, favoring information from neither direction. In upwind and downwind schemes, the derivative is taken using asymmetric information, either favoring the direction toward or the direction away from the source of the flow, e.g., at positions i, $i+1$ or i, $i-1$ at the previous time step.

3. **The model domain.** In this project, we will implement at least a two-dimensional model for the study of Magnetosheath Jets (see section 2).

4. **Accuracy.** The schemes we have chosen are of second- and third-order accuracy.

5. **Divergence cleaning.** At the end of every time iteration, the constraint $\nabla \cdot \mathbf{B} = 0$ must be enforced. To this end we will utilize the Leray projection method.

We now describe several widely-used MHD solvers and briefly list their specifications. GORGON is a finite-volume, three-dimensional, second-order MHD code that is capable of supporting single- or multi-fluid simulations. It has been used to study Z-pinches (Chittenden et al., 2004), Earth's bow shock and plasma jets (Mejnertsen et al., 2018), among other applications. ZEUS is an open-source MHD code. ZEUS uses a finite-differencing method that supports Cartesian, cylindrical, or spherical grids (Stone, 1999). It has been applied to model the plasma flow around Saturn's moon Titan and other astrophysical flows (e.g., Ledvina & Cravens, 1998), as well as plasma jets (e.g., Clarke et al., 1990). BATS-R-US is another open-source MHD code, a part of the Space Weather Modeling Framework (SWMF). BATS-R-US is highly modular, utilizing a finite-volume, upwind derivative scheme, several time-integration schemes, MPI parallel processing, and the choice of Cartesian or curvilinear coordinate systems. It captures complex behavior such as the Hall effect, radiative transport, and heat conduction (Tóth et al., 2012). It has been used to simulate CMEs (Gombosi et al., 2003), to compare against measurements of Saturn's magnetosphere taken by the

Cassini spacecraft (Hansen et al., 2005), and to study the interaction between Europa and its plasma environment (Harris et al., 2021), among many other applications. Tóth et al. (2012) improved upon the BATS-R-US core with BATL to patch some limitations in the original model. For a list of codes comprising the SWMF, refer to Table 1 of that paper. *These are standard test problems*

Balbás et al. (2004) built a one- and two-dimensional MHD solver and applied it to the shock-tube, Kelvin-Helmholtz and Orszag-Tang problems. This study uses second- and third-order central differencing schemes developed by Liu and Tadmor (1998), Jiang and Tadmor (1998) and Nessyahu and Tadmor (1990). We will adapt these methods for this project (see section 3.3).

2 Science Objectives

2.1 Systems of Interest

To capture shocks, you'll need to implement a Riemann solver that treats the up/downwind sides and computes the wave speeds. only try to implement it after getting your MHD solver working

We have identified three systems of interest to investigate in the proposed work: a quasi-1 dimensional shock tube, plasma containment in a Tokamak reactor, and magnetosheath jets. The quasi-1D MHD shock tube, also known a Brio-Wu Shock Tube (Brio & Wu, 1988), is a common test for MHD codes; we will investigate the propagation of shock waves, rarefaction waves, and contact discontinuities from an initial discontinuity in pressure and density. In this case, density (i.e., mass distribution), velocity (flow speed of plasma from initial pressure gradient), magnetic field (influences wave speeds and shock structures), plasma pressure (pressure of the plasma), temperature (to show energy changes), characteristic speeds (slow, fast, Alfvén), and mach number (relation to the MHD wave speeds) will be examined as functions of space (domain $\approx 1\,\mathrm{m}$) and over timescales of ms.

A common practice is to work in dimensionless units instead of SI/cgs.

For a quasi two-dimensional case, we investigate plasma containment in a Tokamak reactor. The goal is to model the equilibrium, stability and dynamics of magnetically confined plasma in torus with azimuthal symmetry. We will focus only on the radial variation in the reactor tube (Chance et al., 1982). Plasma density (shows mass distribution and confinement efficiency), velocity (flow patterns and turbulence-driven transport), magnetic field (responsible for confinement and stability), plasma pressure (balance of thermal and magnetic forces), temperature (energy and fusion reaction rates), current density (equilibrium and stability), magnetic flux surfaces (quality of equilibrium), and pitch of the magnetic field (instead of safety factor) will be inspected and analyzed as functions of space (domain $\approx 10\,\mathrm{m}$) and timescales given by the resistive-diffusive dimensionless parameter.

The final system we consider is magnetosheath jets (Pöppelwerth et al., 2024). In a jet in the magnetosheath region is a collimated population of locally enhanced dynamic pressure. Quantities of interest are plasma density (variations help identify jets), velocity (to show jet flow patterns), magnetic field (influences jet dynamics and stability), plasma pressure (gradients are important to jet formation), current density, and mach number (speed relative to MHD wave modes). All of these quantities will be examined (see Pöppelwerth et al., 2024, for length- & timescales). The proposed work investigates the size and structure of the jet, as well as its sensitivity to the MHD environment.

Science Questions:

1. How does plasma behave in a quasi-1 Dimensional Shock Tube? (Brio & Wu, 1988)
2. How is plasma confined in the Tokamak reactor toroidal geometry? (Chance et al., 1982)
3. How do plasma jets in boundary layers (e.g., the magnetosheath) affect the bulk behavior of transport and convection? (e.g., Pöppelwerth et al., 2024)

3 Technical Approach and Methodology

In this effort, we seek to uncover physical understanding for multiple science questions (see section 2) by implementing a tool that calculates solutions to the ideal MHD system in one, two and (as needed) three dimensions. In section 3.1, we first give a brief overview of the assumptions made to yield the ideal MHD system. Second, we explicitly outline the system of equations that we will

solve numerically in the proposed work in section 3.2. Finally, in section 3.3 we outline the numerical approach of Balbás et al. (2004) used in the proposed work to solve the ideal MHD system.

3.1 Physical Assumptions of Ideal MHD

The ideal MHD framework assumes that the frequency of disturbances (i.e., plasma waves) are small, and that the displacement current is negligible. The setup of the system involves a bulk flow of plasma $\mathbf{u}$ (assuming collective motion of ions and electrons) with some component orthogonal to the ambient magnetic field $\mathbf{B}$. The ideal MHD model also inherently assumes the plasma to be traveling frozen-in to the magnetic field (Alfvén, 1942), and hence a convective electric field $\mathbf{E}$ arises in the rest frame of the plasma. The expression for $\mathbf{E}$ then reads

$$\mathbf{E} = -\mathbf{u} \times \mathbf{B} \qquad . \tag{11}$$

This assumption implies that the ohmic term of the electric field equation (i.e., equation 10) $\eta \mathbf{J}$ is neglected, along with Hall and electron pressure terms.

3.2 The Ideal MHD System

The ideal MHD system (where ρ is the density, p is the scalar pressure, and $\gamma \equiv 2$ is the adiabatic index for a plasma, assumed constant) is given by

$$\partial_t \rho + \nabla \cdot (\rho \mathbf{u}) = 0 \qquad , \tag{12}$$

$$\partial_t (\rho \mathbf{u}) + \nabla \cdot \left[\rho \, \mathbf{u} \otimes \mathbf{u} + \left(p + \frac{\mathbf{B}^2}{2\mu_0} \right) \mathbb{I} - \frac{\mathbf{B} \otimes \mathbf{B}}{\mu_0} \right] = 0 \qquad , \tag{13}$$

$$\partial_t \mathbf{B} = \nabla \times (\mathbf{u} \times \mathbf{B}) \qquad , \tag{14}$$

$$\partial_t \mathcal{E} \equiv \partial_t \left(\frac{\rho \mathbf{u}^2}{2} + \frac{p}{\gamma - 1} + \frac{\mathbf{B}^2}{2\mu_0} + \frac{\epsilon_0 \mathbf{E}^2}{2} \right) = -\nabla \cdot \left[\left(\frac{\rho \mathbf{u}^2}{2} + \frac{\gamma \, p}{\gamma - 1} \right) \mathbf{u} - \frac{\mathbf{E} \times \mathbf{B}}{\mu_0} \right] \qquad , \tag{15}$$

for net internal energy $\mathcal{E}$, with the additional constraint of

$$\nabla \cdot \mathbf{B} = 0 \qquad . \tag{16}$$

The ideal MHD system arises from successively higher order moments (in velocity space) of Vlasov's equation with the Lorentz Force: the continuity equation (i.e., equation (12)) is the zeroth moment, Navier-Stokes equation (i.e., equation (13)) is the first, and the energy equation with no heat flux (i.e., equation (15)) is the second. Additional simplifications can be made to equation (15) using the expression for the convective electric field in equation (11).

While the energy equation is typically included in models that implement MHD to calculate electromagnetic field and plasma properties (e.g., Balbás et al., 2004; Duling et al., 2014; Jia et al., 2009), this treatment can (in many applications) be circumvented by assuming the plasma to be adiabatic. This approximation can still reproduce all four primary linear MHD wave modes (i.e., Alfvén, Fast, Slow, and Entropy modes). Further, this treatment is sufficient to determine the behavior of plasmas at a plasma boundary (i.e., a discontinuity). However, some non-adiabatic processes (e.g., shocks) are not accounted for with this approximation. In the adiabatic regime, the MHD system includes a simple adiabatic law to relate pressure and density, much more tractable than equation (15). That is, this approach assumes the following to hold:

$$p = p_0 \left(\frac{\rho}{\rho_0} \right)^{\gamma} \qquad , \tag{17}$$

where p_0 and ρ_0 are some fixed reference values for the pressure and density, respectively.

Together, equations (12), (13), (14), and (15) constitute a full description of the ideal MHD system, with no assumptions made about the relationship between changes in pressure and density.

However, the set of equations (12), (13), (14), and (17) *also* constitutes a closed system representing ideal MHD. Since the processes we are interested in mainly occur in the adiabatic regime (see section 2), we employ the system of equations: (12), (13), (14), and (17), subject to the constraint (16). ✓

3.3 Numerical Approach

Good approach

In order to numerically calculate approximate solutions to the ideal MHD system, we implement the ideal MHD scheme of Balbás et al. (2004). These authors employ a non-oscillatory, staggered-mesh, predictor-corrector central differencing technique. This approach yields the advantage of *not* requiring the processing of a Jacobian matrix in each timestep, as opposed to the upwind schemes usually employed. The staggered-mesh approach cicrumvents the need to compute the eigenmodes of the Jacobian at each timestep. Here, we outline our approach for the case of one spatial dimension. This treatment is directly extended to two dimensions (see section 3 of Balbás et al., 2004).

The method relies on the similar form of all ideal MHD equations. Aside from equation (17) which we can approximate with a second order finite difference, each of the ideal MHD equations can be written in the form of a conservation law (for some quantity Y describing the plasma):

$$\partial_t Y + f(\nabla, Y) = 0 \qquad . \tag{18}$$

Then, each quantity Y (i.e., $\mathbf{B}, \mathbf{u}, \rho$) can be represented by the *sliding average* $\bar{Y}$ across each cell of width Δx, given by

$$\bar{Y} \equiv \frac{1}{\Delta x} \int_{x - \frac{\Delta x}{2}}^{x + \frac{\Delta x}{2}} Y(x', t) \, \mathrm{d}x' \qquad .$$

For the sliding average of Y, the conservation law (equation (18)) takes the form

$$\bar{Y}(x, t) + \frac{1}{\Delta x} \left(f\left(Y\left(x + \frac{\Delta x}{2}, t \right) \right) - f\left(Y\left(x - \frac{\Delta x}{2}, t \right) \right) \right) = 0 \qquad .$$

By introducing a small timestep Δt, the time evolution can be represented by the equation

$$\bar{Y}(x, t + \Delta t) = \bar{Y}(x, t) - \frac{1}{\Delta x} \int_t^{t + \Delta t} \left[f\left(Y\left(x + \frac{\Delta x}{2}, t' \right) \right) - f\left(Y\left(x - \frac{\Delta x}{2}, t' \right) \right) \right] \mathrm{d}t' \tag{19}$$

✓

At this point in the derivation of our scheme, Balbás et al. (2004) emphasize that the solution is still *exact*. Only does this change with the introduction of a piecewise polynomial approximation $Z(x, t^n) \sim Y(x, t^n)$, defined uniquely for each cell such that the quantity is continuous across each cell. However, the discrete cells upon which each polynomial fit is defined are *staggered*, that is, the Ith staggered cell for the fit function is given by $[x_{i-\frac{1}{2}}, x_{i+\frac{1}{2}}]$. A quadrature technique is employed to approximate the quantities that are integrated in each timestep for higher order solvers, but we follow the approach of Balbás et al. (2004) and use a piecewise linear form to achieve second order accuracy. Hence, the expression solved at each timestep for every quantity (for time $t_n \equiv n\Delta t$) is

$$\bar{Z}_{j+\frac{1}{2}}^{n+1} = \frac{1}{\Delta x} \int_{I_{j+\frac{1}{2}}} Z(x, t_n) \, \mathrm{d}x - \frac{1}{\Delta x} \left[\int_{t^n}^{t^{n+1}} f(w(x_{j+1}, t)) \, \mathrm{d}t - \int_{t^n}^{t^{n+1}} f(w(x_j, t)) \, \mathrm{d}t \right] \qquad . \tag{20}$$

By using a technique of second order to calculate the numerical derivatives of each quantity, we can evaluate equation (20) at each timestep for every point in our domain. This process yields a stable, non-oscillatory scheme for the central finite differences. Further details on this method and its extension to a higher dimension can be found in Balbás et al. (2004). ✓

4 Relevance

Magnetohydrodynamics (MHD) is a fundamental framework for modeling the interaction between fluid dynamics and electromagnetic fields, making it a critical tool in fields such as physics,

geophysics, and astrophysics. Our proposed MHD framework provides a robust method for modeling complex phenomena and uncovering the physics driving these plasma systems.

A notable application of MHD is the modeling of high-energy plasma in stellar structures and the interstellar medium. MHD models help explain the formation and dynamics of stellar interiors, sunspots, corona, solar flares, solar winds, and a large number of similar phenomena. Accurately modeling the interplay between magnetic fields and plasma flows using MHD simulations is key to accurately interpreting observational data and guiding future theoretical predictions. Stellar plasma - especially in regions like the stellar corona and convective-radiative boundary - often exhibit sharp interfaces, shock waves, and highly variable magnetic structures. Conventional numeric simulations often suffer from the Gibbs phenomenon near these discontinuities which can lead to non-physical oscillations that degrade simulation accuracy. Our non-oscillatory MHD framework allows us to more reliably study phenomena like magnetosheath jets (see section 2).

5 Acknowledgements

References

Alfvén, H. (1942, October). Existence of Electromagnetic-Hydrodynamic Waves. *Nature*, *150*(3805), 405-406. doi: 10.1038/150405d0

Balbás, J., Tadmor, E., & Wu, C.-C. (2004, November). Non-oscillatory central schemes for one- and two-dimensional MHD equations: I. *Journal of Computational Physics*, *201*(1), 261-285. doi: 10.1016/j.jcp.2004.05.020

Baumjohann, W., & Treumann, R. A. (1999). *Basic space plasma physics*. Imperial College Press, London.

Brio, M., & Wu, C. (1988). An upwind differencing scheme for the equations of ideal magnetohydrodynamics. *Journal of Computational Physics*, *75*(2), 400-422. Retrieved from https://www.sciencedirect.com/science/article/pii/0021999188901209 doi: https://doi.org/10.1016/0021-9991(88)90120-9

Chance, M., Furth, H., Glasser, A., & Selberg, H. (1982, feb). Ideal- and resistive-mhd stability of one-dimensional tokamak equilibria. *Nuclear Fusion*, *22*(2), 187. Retrieved from https://dx.doi.org/10.1088/0029-5515/22/2/001 doi: 10.1088/0029-5515/22/2/001

Chittenden, J. P., Lebedev, S. V., Jennings, C. A., Bland, S. N., & Ciardi, A. (2004, nov). X-ray generation mechanisms in three-dimensional simulations of wire array z-pinches. *Plasma Physics and Controlled Fusion*, *46*(12B), B457. Retrieved from https://dx.doi.org/10.1088/0741-3335/46/12B/039 doi: 10.1088/0741-3335/46/12B/039

Clarke, D. A., Stone, J. M., & Normal, M. (1990). Mhd jet simulations in three dimensions.

Dorelli, J. C., Glocer, A., Collinson, G., & Tóth, G. (2015). The role of the Hall effect in the global structure and dynamics of planetary magnetospheres: Ganymede as a case study. *Journal of Geophysical Research A: Space Physics*, *120*(7), 5377–5392. doi: 10.1002/2014JA020951

Duling, S., Saur, J., & Wicht, J. (2014). Consistent boundary conditions at nonconducting surfaces of planetary bodies: Applications in a new Ganymede MHD model. *Journal of Geophysical Research: Space Physics*, *119*(6), 4412–4440. doi: 10.1002/2013JA019554

Fatemi, S., Holmstrm, M., & Futaana, Y. (2012). The effects of lunar surface plasma absorption and solar wind temperature anisotropies on the solar wind proton velocity space distributions in the low-altitude lunar plasma wake. *Journal of Geophysical Research: Space Physics*, *117*(10), 1–13. doi: 10.1029/2011JA017353

Fatemi, S., Poppe, A., Khurana, K., Holmström, M., & Delory, G. (2016). On the formation of Ganymede's surface brightness asymmetries: Kinetic simulations of Ganymede's magnetosphere. *Geophysical Research Letters*, *43*(10), 4745–4754. doi: 10.1002/2016GL068363

Gombosi, T. I., De Zeeuw, D. L., Powell, K. G., Ridley, A., Sokolov, I. V., Stout, Q. F., & Tóth,

G. (2003). Adaptive Mesh Refinement for Global Magnetohydrodynamic Simulation. In J. Büchner, C. T. Dum, & M. Scholer (Eds.), *Space Plasma Simulation* (pp. 247–274). Springer-Verlag, Berlin/ Heidelberg/ New York.

Hansen, K. C., Ridley, A. J., Hospodarsky, G. B., Achilleos, N., Dougherty, M. K., Gombosi, T. I., & Toth, G. (2005). Global MHD simulations of Saturn's magnetosphere at the time of Cassini approach. *Geophysical Research Letters*, *32*(20), L20S06 (1–5).

Harris, C. D. K., Jia, X., Slavin, J. A., Toth, G., Huang, Z., & Rubin, M. (2021). Multi-Fluid MHD Simulations of Europa's Plasma Interaction Under Different Magnetospheric Conditions. *Journal of Geophysical Research: Space Physics*, *126*(5), e2020JA028888. Retrieved from `https://agupubs.onlinelibrary.wiley.com/doi/abs/10.1029/2020JA028888` (e2020JA028888 2020JA028888) doi: https://doi.org/10.1029/2020JA028888

Jia, X., Walker, R. J., Kivelson, M. G., Khurana, K. K., & Linker, J. A. (2009). Properties of Ganymede's magnetosphere inferred from improved three-dimensional MHD simulations. *Journal of Geophysical Research: Space Physics*, *114*(9). doi: 10.1029/2009JA014375

Jiang, G.-S., & Tadmor, E. (1998). Nonoscillatory central schemes for multidimensional hyperbolic conservation laws. *SIAM Journal on Scientific Computing*, *19*(6), 1892-1917. Retrieved from `https://doi.org/10.1137/S106482759631041X` doi: 10.1137/S106482759631041X

Ledvina, S., & Cravens, T. (1998). A three-dimensional mhd model of plasma flow around titan. *Planetary and Space Science*, *46*(9), 1175-1191. Retrieved from `https://www.sciencedirect.com/science/article/pii/S003206339800052X` doi: https://doi.org/10.1016/S0032-0633(98)00052-X

Lipatov, A. S., Motschmann, U., Bagdonat, T., & Griessmeier, J. M. (2005). The interaction of the stellar wind with an extrasolar planet – 3D hybrid and drift-kinetic simulations. *Planetary and Space Science*, *53*, 423–432.

Liu, X.-d., & Tadmor, E. (1998, 11). Third order nonoscillatory central scheme for hyperbolic conservation laws. *Numerische Mathematik*, *79*. doi: 10.1007/s002110050345

Mejnertsen, L., Eastwood, J. P., Hietala, H., Schwartz, S. J., & Chittenden, J. P. (2018). Global mhd simulations of the earth's bow shock shape and motion under variable solar wind conditions. *Journal of Geophysical Research: Space Physics*, *123*(1), 259-271. Retrieved from `https://agupubs.onlinelibrary.wiley.com/doi/abs/10.1002/2017JA024690` doi: https://doi.org/10.1002/2017JA024690

Müller, J., Simon, S., Motschmann, U., Schüle, J., Glassmeier, K. H., & Pringle, G. J. (2011). A.I.K.E.F.: Adaptive hybrid model for space plasma simulations. *Computer Physics Communications*, *182*(4), 946–966. Retrieved from `http://dx.doi.org/10.1016/j.cpc.2010.12.033` doi: 10.1016/j.cpc.2010.12.033

Nessyahu, H., & Tadmor, E. (1990). Non-oscillatory central differencing for hyperbolic conservation laws. *Journal of Computational Physics*, *87*(2), 408-463. Retrieved from `https://www.sciencedirect.com/science/article/pii/0021999190902608` doi: https://doi.org/10.1016/0021-9991(90)90260-8

Pöppelwerth, A., Glebe, G., Mieth, J. Z. D., Koller, F., Karlsson, T., Vörös, Z., & Plaschke, F. (2024). Scale size estimation and flow pattern recognition around a magnetosheath jet. *Annales Geophysicae*, *42*(1), 271–284. Retrieved from `https://angeo.copernicus.org/articles/42/271/2024/` doi: 10.5194/angeo-42-271-2024

Stone, J. M. (1999, May). The ZEUS code for astrophysical magnetohydrodynamics: new extensions and applications. *Journal of Computational and Applied Mathematics*, *109*, 261-280.

Stone, J. M., & Norman, M. L. (1992, June). ZEUS-2D: A Radiation Magnetohydrodynamics Code for Astrophysical Flows in Two Space Dimensions. I. The Hydrodynamic Algorithms and Tests. *American Journal of Physical Science*, *80*, 753. doi: 10.1086/191680

Tóth, G., van der Holst, B., Sokolov, I. V., De Zeeuw, D. L., Gombosi, T. I., Fang, F., ... Opher, M. (2012). Adaptive numerical algorithms in space weather modeling. *Journal of Computational Physics*, *231*(3), 870-903. Retrieved from `https://www.sciencedirect.com/science/article/pii/S002199911100088X` (Special Issue: Computational Plasma Physics) doi: https://doi.org/10.1016/j.jcp.2011.02.006

Winske, D., & Omidi, N. (1996). A nonspecialist's guide to kinetic simulations of space plasmas. *Journal of Geophysical Research: Space Physics*, *101*(A8), 17,287–17,303.